Analytica Chimica Acta 1416 (2026) 345714

Contents lists available at ScienceDirect

Analytica Chimica Acta

journal homepage: www.elsevier.com/locate/aca

A "signal-on" electrochemical sensor for the rapid hyaluronidase activity detection in biologics and urine samples

Wan-Yue Zhuang [a], Xingdong Yang [a], Sen Zhang [a], Zi-Yi Wang [a], Chen-Hui Liu [a], Jun-Qin Qiao [a,*], Wei-Juan Zheng [b], Hong-Zhen Lian [a,**]

[a] State Key Laboratory of Analytical Chemistry for Life Science, School of Chemistry & Chemical Engineering and Centre for Shared Scientific Research Facilities, Nanjing University, 163 Xianlin Avenue, Nanjing, 210023, China
[b] State Key Laboratory of Pharmaceutical Biotechnology, School of Life Sciences, Nanjing University, 163 Xianlin Avenue, Nanjing, 210023, China

HIGHLIGHTS

- A dual-scene electrochemical sensor is developed to quantify hyaluronidase activity.
- Homogeneous electrochemical strategy enhanced the signal stability and repeatability.
- The novel sensor enables efficient detection of hyaluronidase activity within 15 min.
- Provide a tool for both quality control and clinical diagnostics of hyaluronidase.

GRAPHICAL ABSTRACT

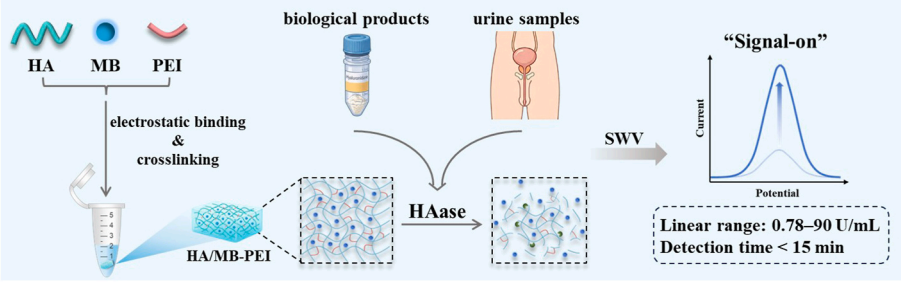

ARTICLE INFO

Handling Editor: Dr Jing-Juan Xu

Keywords:
Hyaluronidase activity
Electrochemical sensor
Enzyme-responsive hydrogel
Pharmaceutical quality control
Non-invasive clinical screening

ABSTRACT

Background: Hyaluronidase (HAase) is a clinically important glycosidase that functions both as a drug diffusion enhancer and a disease biomarker. The quantification of HAase activity in biopharmaceutical products has received limited attention and still relies on conventional methods. Furthermore, the rapid and accurate determination of HAase activity is of great significance for cancer diagnosis and could facilitate the development of non-invasive examination methods. These considerations highlight the urgent demand for developing novel, rapid and accurate strategies for detecting HAase activity.

Results: In this work, we developed a "signal-on" electrochemical sensor based on an enzyme-responsive hydrogel for the sensitive and rapid detection of HAase activity. The sensor was constructed by crosslinking hyaluronic acid (HA) and polyethylenimine (PEI) to form a hydrogel that electrostatically encapsulates methylene blue (MB). HAase-triggered hydrogel degradation releases MB, generating a measurable current increase. The results demonstrated a strong linear relationship ($R^2 = 0.9973$) between the change in current and HAase activity within the range of 0.78–90 U/mL, with a limit of detection of 0.48 U/mL. The sensor exhibits good specificity, repeatability, and storage stability. Moreover, the sensor has been successfully applied to the analysis of bio-pharmaceutical products and human urine samples.

Significance: This facile electrochemical sensor is capable of addressing both drug quality control and disease monitoring. With rapid detection in just 15 min, it significantly improves the efficiency of drug quality

* Corresponding author.
** Corresponding author.
E-mail addresses: qiaojunqin@nju.edu.cn (J.-Q. Qiao), hzlian@nju.edu.cn (H.-Z. Lian).

https://doi.org/10.1016/j.aca.2026.345714
Received 12 April 2026; Received in revised form 20 May 2026; Accepted 25 May 2026
Available online 26 May 2026

evaluation and disease diagnosis. This innovative approach offers a promising tool for the quality evaluation of HAase pharmaceuticals and their diagnostic monitoring.

1. Introduction

Hyaluronidase (HAase) is a glycosidase widely distributed in animals and microorganisms [1–3] and plays a crucial role in various physiological and pathological processes [4]. Hyaluronic acid (HA), a major component of the extracellular matrix (ECM), serves as the primary substrate of HAase. By hydrolyzing HA, HAase reduces tissue viscosity and enhances tissue permeability [5], which enables its use as an effective spreading factor in clinical activities [6]. HAase also functions as a significant indicator for the development of bladder cancer and has been proven to be significantly elevated in the urine of bladder cancer patients [7,8]. While cystoscopy remains the clinical gold standard for bladder cancer diagnosis, its invasiveness and the resulting physical pain often lead to poor patient compliance during long-term surveillance [9,10]. This necessitates the development of non-invasive diagnostic alternatives, such as urine-based methods, which can bridge the gap between diagnostic precision and patient comfort. Given its dual function as both a therapeutic agent and a disease biomarker, accurate monitoring of HAase activity is critically important. For biopharmaceutical applications, the efficacy and safety of HAase drugs are highly dependent on their enzymatic activity, which is prone to inactivation during transportation and storage [11]. Rapid activity assays prior to use provide timely quality assessment, ensuring drug safety and therapeutic effectiveness. Similarly, in clinical diagnostics, fast and accurate detection of HAase activity in biological samples can improve diagnostic efficiency, facilitating earlier disease intervention and improved patient management. Therefore, the accurate and rapid quantification of HAase activity is crucial for both pharmaceutical quality control and clinical diagnosis.

A variety of methods have been established for the assay of HAase activity. Traditional techniques such as the turbidimetric [12] and viscosimetric methods [13] have long been used, with the former being adopted as the standard method by both the Chinese Pharmacopoeia (CP) [14] and the United States Pharmacopoeia (USP). Although these approaches enable accurate determination of enzyme activity, they generally involve tedious procedures and require lengthy processing times, making them unsuitable for on-site rapid testing. In recent years, several novel methods, such as colorimetry [15,16], fluorescence spectrometry [17], surface-enhanced Raman spectroscopy (SERS) [18,19], electrochemiluminescence (ECL) [20–22] and photoelectrochemical techniques [23,24], have been exploited for the determination of HAase activity in complex biological samples. However, the rapid measurement of HAase activity in biopharmaceutical products has received relatively limited attention. Consequently, there is a pressing need for a detection platform capable of rapidly and reliably detecting HAase activity applicable to both biopharmaceutical products and complex biological samples.

Electrochemical methods present notable advantages for sensing and detection owing to their operational simplicity, low instrument cost, and quick response [25,26]. However, they typically require the immobilization of biorecognition elements onto the electrode's surface [27], which is not only laborious and time-consuming but also suffers from poor reproducibility of electrode modification [28]. Homogeneous electrochemistry presents a promising alternative strategy to overcome this limitation. By transferring the heterogeneous reactions occurring at the electrode surface into homogeneous reactions in solution, it enables direct detection of electrochemical signals from electroactive species, thereby improving the reliability of electrochemical sensors [29,30]. A powerful approach to constructing homogeneous electrochemical sensors involves the use of stimulus-responsive materials to encapsulate electroactive molecules [31]. In this strategy, the target analyte acts as a stimulus to trigger the responsive materials, leading to the release or exposure of the encapsulated electroactive probes. The concentration or activity of the target analyte can be sensitively and quantitatively determined by monitoring the signal of the released electroactive probes, which correlates straightway with the analyte. Therefore, constructing a homogeneous electrochemical sensor based on HA hydrogel may be a promising method for HAase activity detection.

Methylene blue (MB), a widely utilized cationic electroactive dye, can efficiently bind to negatively charged molecules via electrostatic interactions [32]. HA, as an excellent hydrogel precursor, possesses strong polyanionic characteristics owing to its abundant carboxyl groups, enabling the stable encapsulation of cationic species such as MB. Based on this principle, we developed a rapid electrochemical sensor for detecting HAase activity, utilizing an enzyme-responsive hydrogel. The activity of HAase was quantified by directly measuring the electrochemical signal of MB in the supernatant and comparing it to enzyme-free controls. The entire assay can be completed within 15 min. This electrochemical sensor has been successfully applied to the quantitative detection of HAase activity in both biopharmaceutical products and human urine samples, demonstrating its potential for broad practical applications.

2. Experimental section

2.1. Reagents and materials

Hyaluronidase (HAase, from bovine testes, ≥300 U/mg), chymotrypsin (Chy), hyaluronic acid sodium salt (HA, from *Streptococcus equi*), N-hydroxysuccinimide (NHS), potassium dihydrogen phosphate (KH_2PO_4) and dipotassium hydrogen phosphate (K_2HPO_4) were all purchased from Shanghai Aladdin Biochemical Technology Co., Ltd. (Shanghai, China). Potassium hyaluronate (from the cockscomb flower), methylene blue (MB), polyethylenimine (PEI), 1-(3-(dimethylamino) propyl)-3-ethylcarbodiimide hydrochloride (EDC), sodium dihydrogen phosphate (NaH_2PO_4), disodium hydrogen phosphate (Na_2HPO_4), sodium chloride (NaCl), potassium chloride (KCl), gelatin, mannitol, urea, acetic acid and L-alanine (L-Ala) were all acquired from Shanghai Macklin Biochemical Co., Ltd. (Shanghai, China). Potassium acetate was obtained from Meryer Chemical Technology Co., Ltd. (Shanghai, China). HAase certified reference material (CRM) was provided by the National Institutes for Food and Drug Control (NIFDC, Beijing, China). HAase testing samples were obtained from commercially available products. Fetal bovine serum (FBS) was purchased from Gibco (Waltham, MA, USA). Thrombin (Tb, 5000 U) was purchased from Nanjing Dulai Biotechnology Co., Ltd. (Nanjing, China). Peptide-N-Glycosidase F (PNGase F) and O-Glycosidase were obtained from New England Biolabs (Ipswich, MA, USA). All aqueous solutions were prepared using ultrapure water (18.2 MΩ cm resistivity) purified through a Milli-Q water purification system (Millipore, Billerica, MA, USA). PBS (0.01 M) was prepared by mixing 0.01 M K_2HPO_4 and 0.01 M KH_2PO_4, both containing 0.01 M KCl, and adjusting the pH to 7.40. Human urine samples were provided by healthy volunteers from Nanjing University and bladder cancer patients from The First Affiliated Hospital of Nanjing Medical University, approved by the Medical Ethical Committees of Nanjing University and The First Affiliated Hospital of Nanjing Medical University respectively. All urine samples were aliquoted and stored frozen for later use. For the spike-recovery experiment, the urine samples were freshly spiked with HAase before experiments.

2.2. Apparatus

Square wave voltammetry (SWV) experiment was performed using a CHI660E electrochemistry workstation (Chenhua, Shanghai, China) and a screen-printed carbon electrode (model: TC201, Poten, Weihai, China). The electrode consisted of carbon ink working and counter electrodes, an Ag/AgCl reference electrode, and a PET substrate. No additional activation procedures or pretreatment were applied before use. The incubator was purchased from Shanghai Lichen Instrument Technology Co., Ltd. The water bath was bought from Faithful Instruments Co., Ltd. (Hebei, China). Zeta potential measurements were performed on a Malvern Panalytical Zetasizer Nano Z instrument (Malvern, UK). UV-vis measurements were conducted on a Hitachi UH5300 spectrophotometer (Hitachi, Tokyo, Japan). Scanning electron microscopy (SEM) images were taken on a Hitachi S4800 microscope (Hitachi, Tokyo, Japan). Fourier-transform infrared (FT-IR) spectra with attenuated total reflection (ATR) mode were collected on a Nicolet iS50 FTIR spectrometer (Thermo-Fisher, Waltham, MA, USA).

2.3. Fabrication of HA/MB-PEI hydrogel

HA sodium salt solution (60 μL, 1%) was mixed with EDC solution (10 μL, 48.8 mg/mL), NHS solution (10 μL, 11.5 mg/mL) and MB solution (10 μL, 1.5 mg/mL) in a 500 μL centrifuge tube. The mixture was shaken for 30 min to activate carboxylic group of HA and form HA/MB complex. Subsequently, PEI solution (40 μL, 0.5%) was added and reacted with activated HA for 5 h. Following this reaction, hydrogels formed inside the centrifuge tube via chemical bonding between HA and PEI. Then, the excess reaction solution was removed, and the resulting hydrogel was washed three times. In each wash, 200 μL of deionized water was added, followed by vortexing for 5 s. The wash solution was then removed. This procedure ensured the removal of surface-adsorbed MB. Finally, the prepared HA/MB-PEI hydrogel was stored at 4 °C for further use.

2.4. Electrochemical detection of HAase activity

A volume of 100 μL of HAase solution (0.01 M PBS: 0.01 M K_2HPO_4/KH_2PO_4, 0.01 M KCl, pH 7.40) was applied to the HA/MB-PEI hydrogel and incubated at 37 °C for 10 min to hydrolyze the hydrogel, resulting in the release of MB. Subsequently, 50 μL of the collected reaction solution was applied to a screen-printed carbon electrode for square wave voltammetry (SWV) measurement over a potential window of −0.8 to 0 V. The 0.01 M PBS blank control was processed using the same procedure as that of HAase.

3. Results and discussions

3.1. Principle of the electrochemical detection of HAase activity

The mechanism of the electrochemical sensor for detecting HAase activity was illustrated in Scheme 1. Initially, the carboxyl groups of HA were activated by EDC and NHS, enabling an amidation reaction with the amino groups of PEI to form a cross-linked hydrogel. During this activation process, the positively charged electrochemical molecule MB was encapsulated within the hydrogel through electrostatic interaction. After washing, a blue HA/MB-PEI hydrogel was obtained. In the absence of HAase, the hydrogel structure was intact, with minimal release of MB into the solution. In contrast, when HAase was present, it specifically degraded the glycosidic bond of HA, causing disintegration of the hydrogel and the subsequent release of encapsulated MB into the solution. Therefore, by measuring the current variation before and after the addition of HAase, a straightforward correlation can be established between the change of current and HAase activity, allowing quantitative determination of HAase activity.

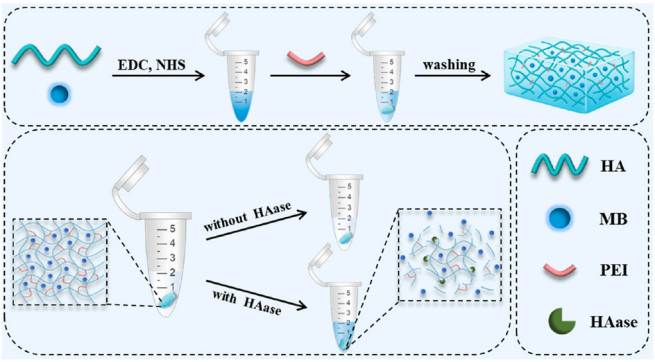

Scheme 1. Principle of the electrochemical detection of HAase activity.

3.2. Verification and characterization of the proposed hydrogel

The feasibility of the proposed method for detecting HAase activity was first investigated. As shown in Fig. 1A, the addition of HAase led to the degradation of HA, producing a distinct color change in the supernatant. The electrochemical signals of supernatant before and after enzymatic reaction were presented in Fig. 1B. Incubation of HA/MB-PEI hydrogel in PBS yielded only a low background signal. Interestingly, the addition of HAase triggered a markedly enhanced SWV response. This significant difference in currents confirms that the electrochemical response is directly driven by HAase activity, thereby validating the feasibility of the sensing method.

Zeta potential measurements of HA, MB, HA/MB, PEI and HA/MB-PEI were carried out in ultrapure water (Fig. 1C). HA exhibited a characteristic negative potential of −29.1 mV due to its abundant carboxyl groups. MB, as a typical cationic dye, carries a positive charge of +0.97 mV in water. After the incorporation of MB, the zeta potential of HA/MB increased to −23.1 mV, indicating the electrostatic interaction between negatively charged HA and the positively charged MB and confirming the encapsulation of MB within the hydrogel. PEI is rich in amino groups, rendering it positively charged in aqueous solution (+1.74 mV). Upon crosslinking HA/MB with PEI, the zeta potential of HA/MB-PEI shifted from negative to positive (+9.9 mV). The observed charge transitions in zeta potential provide clear evidence for the synthesis of the hydrogel.

The morphology of the HA/MB-PEI hydrogel was characterized using scanning electron microscopy (SEM). As shown in Fig. S1, the hydrogel presented a complex and irregular porous structure, forming an integrated three-dimensional network, indicative of a continuous scaffold structure. To further verify the synthesis of the hydrogel, ATR-FT-IR spectroscopy was performed (Fig. 1D). In the spectrum of HA, the broad peak around 3286 cm^{-1} originated from the O–H stretching vibration. The characteristic absorption peaks at 1603 and 1409 cm^{-1} were attributed to asymmetric and symmetric stretching vibrations of carboxylate anions, respectively. While the peak of HA at 1028 cm^{-1} corresponded to the C–O stretching vibration of sugar rings. For PEI, distinct C–H stretching vibrations arising from its carbon backbone appeared at 2928 and 2808 cm^{-1}, while the peaks at 3282 and 1596 cm^{-1} corresponded to the N–H stretching and bending vibrations, respectively. In addition, the absorption peak at 1453 cm^{-1} was assigned to C–N stretching vibration. Notably, the hydrogel spectrum exhibited new peaks at 1636 cm^{-1} (amide I, C═O stretching) and 1565 cm^{-1} (amide II, N–H bending), indicating the formation of amide bonds. Meanwhile, the disappearance of the 1603 cm^{-1} peak, the weakening of the 1409 cm^{-1} band, and the absence of the N–H absorption at 1596 cm^{-1} collectively confirmed the occurrence of an amidation reaction between HA and PEI, thereby verifying the successful synthesis of the hydrogel.

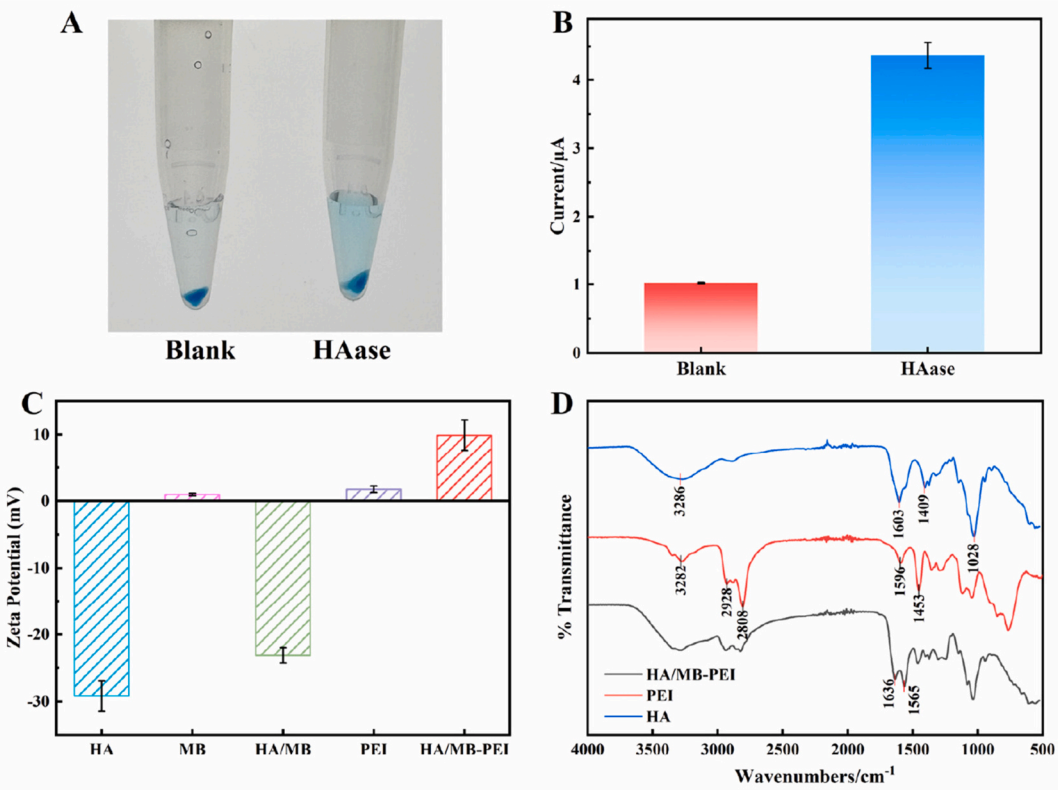

Fig. 1. (A) Photographs of enzyme-responsive HA/MB-PEI hydrogel incubated without (left) and with (right) 50 U/mL HAase; (B) SWV signal of control group and experimental group (50 U/mL HAase) detected by the proposed hydrogel biosensor (n = 3); (C) Zeta potential of HA (blue), MB (pink), HA/MB (green), PEI (purple) and HA/MB-PEI (red) (n = 3); (D) ATR-FT-IR spectra of HA, PEI and the HA/MB-PEI hydrogel. (For interpretation of the references to color in this figure legend, the reader is referred to the Web version of this article.)

3.3. Optimization of the experimental conditions

To enhance sensing performance, several key parameters were systematically optimized. As a crosslinking agent for hydrogel, the mass fraction of PEI directly affects the stability of the hydrogel. Therefore, different mass fractions of PEI were used in the synthesis of the hydrogel in order to determine the optimal condition. As shown in Fig. 2A, an excessively low PEI mass fraction (e.g., 0.1%) resulted in insufficient MB encapsulation and weak electrochemical signals even after enzymatic treatment. As the PEI mass fraction increased from 0.1% to 0.5%, crosslinking was enhanced, improving the encapsulation of MB and inducing a significantly higher current variation. However, when the PEI mass fraction was further increased to 1.0%, the current variation decreased, as a result of the excessive PEI content increasing the crosslinking density and thereby hindering MB release within the given enzymolysis time. Based on these results, a PEI mass fraction of 0.5%, which produced the greatest current variation, was selected as the optimal condition for the synthesis of the hydrogel.

The concentration of MB is another key parameter influencing detection performance, as it straightway determines the level of electrochemical peak current. Therefore, hydrogels were prepared using various concentrations of MB solutions and were subjected to electrochemical detection under reaction with HAase (Fig. 2B). When the concentration of MB was below 1.0 mg/mL, only weak current responses were observed regardless of whether the enzymatic reaction was carried out or not. As the concentration increased to 1.0 mg/mL, the current variation rose in a concentration-dependent enhancement and reached a plateau at 2.5 mg/mL. It is worth noting that when MB concentrations exceeded 2.5 mg/mL, significant MB leakage occurred, resulting in a high background signal. Although the absolute current variation at 2 mg/mL was higher than that at 1.5 mg/mL, the signal-to-background ratio was lower (S/B = 3.4 at 2 mg/mL vs. 4.3 at 1.5 mg/mL). Therefore, 1.5 mg/mL was selected as the optimal MB concentration, making it the optimal choice by balancing high response intensity against low background interference.

Temperature and pH are also important factors influencing the activity of HAase and its enzymatic reaction. Accordingly, the effects of temperature and pH on the hydrolysis of the hydrogel were systematically evaluated. As shown in Fig. 2C, the current variation induced by the enzymatic reaction gradually increased as the temperature rose from 27 °C to 37 °C, reaching a maximum at 37 °C, and then decreased. It is indicated that the physiological temperature of 37 °C is more suitable for the enzymatic hydrolysis of hydrogels by HAase. The influence of pH on the enzymatic hydrolysis reaction was similar to that of temperature, and the result is shown in Fig. 2D. As the pH increased from 6.20 to 7.40, the current variation caused by enzymatic hydrolysis became increasingly significant, reaching a maximum value at pH 7.40, and then decreased at higher pH values. The results suggested that the activity of HAase toward the HA/MB-PEI hydrogel is relatively low under acidic or alkaline conditions but highest under physiological conditions. Therefore, 37 °C with a pH of 7.40 were determined to be the optimal condition for the reaction.

3.4. Analytical performance

Under the optimized experimental conditions, we measured the current of supernatants collected from HA/MB-PEI hydrogels after treatment with different activity concentrations of HAase, and the SWV curves were displayed in Fig. 3A. In the absence of HAase (0 U/mL), the lowest background current was observed. As the HAase activity concentration increased from 0 U/mL to 90 U/mL, a correspondingly greater amount of MB was released from the hydrogel, resulting in a

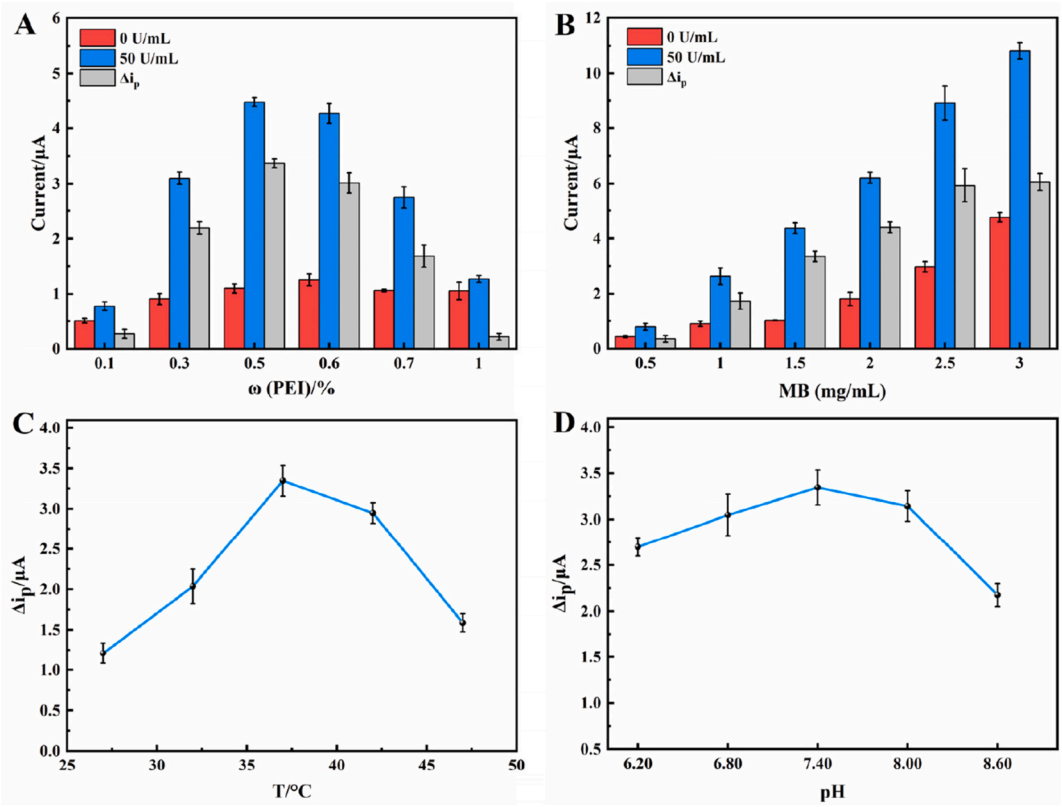

Fig. 2. (A) The relationship between the current signal and mass fraction of PEI (n = 3); (B) The relationship between the current signal and mass concentration of MB (n = 3); (C) The relationship between the current variation and the temperature in enzymatic reaction (n = 3); (D) The relationship between the current variation and the pH in enzymatic reaction (n = 3).

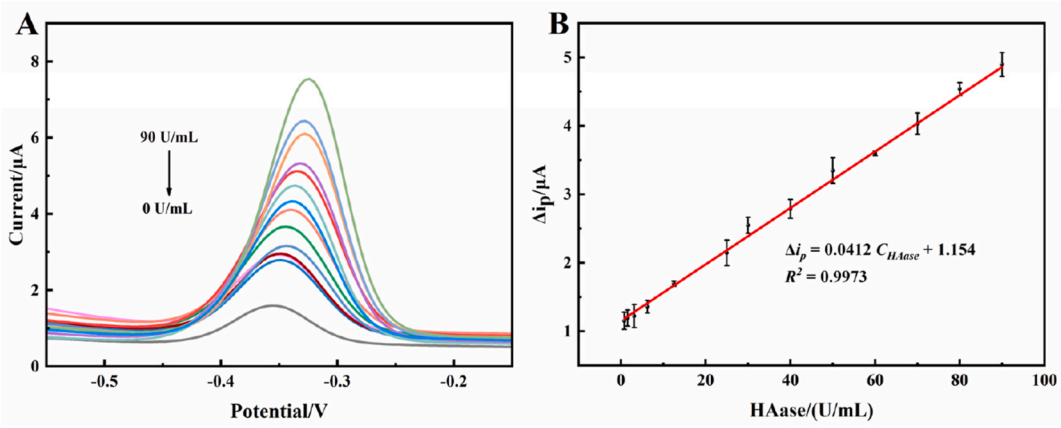

Fig. 3. (A) SWV curves toward various HAase activities (0–90 U/mL); (B) The linear relationship between HAase activity and current variation (n = 3).

gradual increase in the SWV peak current. Additionally, it can be seen that the oxidation peak potential of MB shifted positively with increasing HAase activity, which is in agreement with earlier reports [33,34]. The possible reasons for the shift of oxidation peak potential mainly arise from changes in the physicochemical environment of the supernatant during hydrogel degradation. As the HAase activity increased, larger amounts of MB were released into the supernatant, which may enhance intermolecular interactions or lead to aggregation of MB molecules, resulting in a higher oxidation potential. In addition, HAase and hydrogel degradation fragments were not removed from the supernatant before electrochemical measurement. Thus, the presence of proteins and glycans may impede electron transfer of MB and contribute to the observed positive shift in oxidation potential.

The change in SWV peak current (Δi_p) of the supernatant before and after enzymatic hydrolysis was calculated as $\Delta i_p = i - i_0$, where i_0 was the peak current without HAase, and i was the peak current at a given HAase activity. The relationship between Δi_p and HAase activity was established as shown in Fig. 3B. A linear correlation was observed within the HAase activity range of 0.78–90 U/mL, which could be described by the equation: $\Delta i_p = 0.0412\ C_{HAase} + 1.154$ ($R^2 = 0.9973$). The limit of detection (LOD) was calculated to be 0.48 U/mL (LOD = $3\sigma/s$, where "σ" represented the standard deviation of blank solution, and "s" represented the slope of the calibration plot). The analytical performance of this hydrogel-based assay was compared with previously reported methods for HAase activity detection, as summarized in Table S1. It could be seen that the proposed platform exhibited a wider linear range

and a shorter detection time while maintaining a comparable LOD, highlighting its advantages for rapid and sensitive HAase activity detection.

The reproducibility of the hydrogel was evaluated by comparing the enzymatic hydrolysis results across five consecutively prepared batches. As shown in Fig. S2, the current variation after treatment with 50 U/mL HAase was consistent among the five batches, with a relative standard deviation (RSD) of 4.2%, confirming the good reproducibility of the hydrogel preparation method. Potential interfering substances were selected and tested to evaluate the specificity of the developed method, including sodium chloride (NaCl), potassium chloride (KCl), urea, L-alanine (L-Ala), mannitol, bovine serum albumin (BSA), O-Glycosidase, Peptide-N-Glycosidase F (PNGase F), chymotrypsin (Chy) and thrombin (Tb). As illustrated in Fig. 4, all interfering substances exhibited low current responses with peak currents close to the blank signal, while HAase treatment induced a significant current increase. This distinct signal contrast demonstrated the high specificity of the hydrogel toward HAase, verifying the method's reliability for accurate HAase activity detection in complex matrices. The storage stability of the hydrogel was evaluated by monitoring changes in current after 1, 3, 7, 14 and 28 days of storage. As displayed in Fig. S3, the Δip values retained similar responses to those of freshly prepared hydrogels over a 28-day storage period at 4 °C, indicating that the hydrogel can be stored stably for at least 28 days without compromising sensor performance.

3.5. Confirmation of the electrochemical method with ChP method

To comprehensively assess the applicability of the electrochemical HAase activity sensor in biopharmaceutical quality control, parallel measurements were performed on HAase biologics using both the developed electrochemical method and the official assay described in the Chinese Pharmacopoeia (2020 edition, Part IV, Method 1207). The standard calibration curve of the ChP method is shown in Fig. S4. As summarized in Table 1, the electrochemical method demonstrated comparable accuracy to the ChP method. It also exhibited improved precision, as reflected by lower RSDs. A paired sample Wilcoxon signed-rank test yielded a p-value of 0.225 (>0.05), indicating no statistically significant difference between the two groups of measured values. These findings collectively validate the feasibility of the established sensor for applications in biopharmaceutical quality control and therapeutic monitoring.

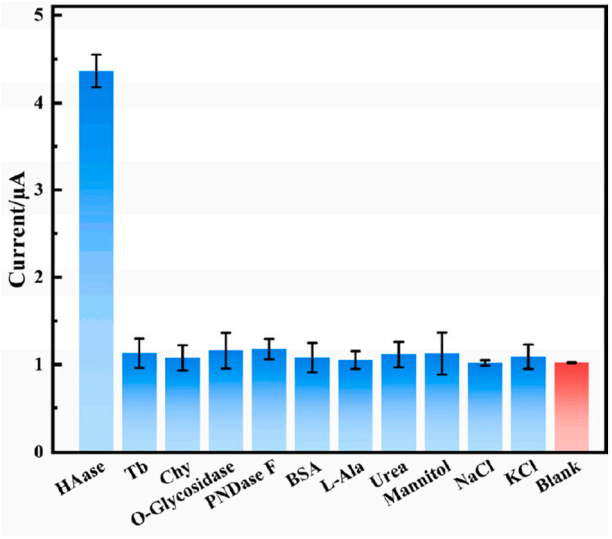

Fig. 4. Peak current of hydrogels corresponding to the addition of 50 U/mL HAase and interfering substances (n = 3).

Table 1
Results of HAase activity using the proposed electrochemical method and the ChP method (n = 3).

No.	Specifications/ (U/mg)	This work		ChP	
		Potency/(U/mg)	RSD/%	Potency/(U/mg)	RSD/%
1	≥300	295.1 ± 19.0	6.5	327.7 ± 24.2	7.4
2	417	408.1 ± 12.2	3.0	387.0 ± 15.2	3.9
3	3521.6	3502.4 ± 122.3	3.5	4011.1 ± 404.0	10.1
4	376	390.7 ± 17.1	4.4	445.0 ± 24.0	5.4
5	798	733 ± 13.7	1.9	731.8 ± 51.6	7.1

3.6. Application of the proposed biosensor in human urine samples

To evaluate the accuracy and precision of the proposed method, spike-recovery experiments were conducted using urine samples which were collected from two healthy volunteers and two bladder cancer patients. The samples were centrifuged at 10,000 rpm for 10 min, and the supernatant was used for the test. The procedure for detecting HAase activity in urine samples followed the same protocol as that used for PBS in the blank control experiment. As shown in Table 2, no endogenous HAase activity was detected in healthy people, but significantly elevated in the urine of bladder cancer patients, which is consistent with previous reports [18,35]. Upon spiking, the detected HAase activities correlated well with the spiked amounts, with recoveries ranging from 87.8% to 101.8% and RSDs between 0.3% and 8.6%. These results confirm that the sensor is sufficiently robust to detect HAase within the concentration ranges typically found in clinical samples [16,36]. Consequently, the hydrogel-based sensor offers a practical and reliable approach for rapid HAase activity monitoring in urine samples.

4. Conclusions

In summary, we presented an electrochemical sensing platform based on an enzyme-responsive HA/MB-PEI hydrogel for the quantification of HAase activity in two distinct application scenarios. The optimal sensing conditions were established as follows: 1.5 mg/mL MB, 0.5% PEI, enzymatic hydrolysis at pH 7.40 and 37 °C. Under these conditions, the sensor exhibited a linear detection range from 0.78 to 90 U/mL, with a detection limit of 0.48 U/mL. The effectiveness of this sensor has been successfully validated in HAase biological products and human urine samples, demonstrating its strong potential for dual-scene applications in both pharmaceutical quality control and clinical diagnostics. Compared with previous reports, the present method enables rapid detection within 15 min, offering the potential for on-site

Table 2
Determination of the HAase activity in human urine samples (n = 3).

Samples		Added/(U/mL)	Found/(U/mL)	Recovery/%	RSD/%
Healthy volunteers	Female	0	ND	/	/
		2	2.0	100.3	5.1
		5	4.4	87.8	3.2
		10	10.2	101.8	8.6
	Male	0	ND	/	/
		2	1.9	94.4	7.0
		5	4.9	97.6	2.5
		10	9.9	98.7	0.3
Bladder cancer patients	Female	0	25.3	/	7.8
		10	34.9	96.1	3.3
		20	44.3	95.2	6.6
		40	65.7	101.2	3.7
	Male	0	38.0	/	3.0
		10	47.9	99.1	5.0
		20	57.0	95.2	3.1
		40	78.3	100.9	3.5

ND: not detected.

detection. In addition, it requires simpler handling which only needs dissolution and dilution. These features highlight the practical value of this method for rapid HAase detection in different real-sample settings.

CRediT authorship contribution statement

Wan-Yue Zhuang: Data curation, Formal analysis, Investigation, Methodology, Validation, Visualization, Writing – original draft. **Xingdong Yang:** Investigation, Methodology. **Sen Zhang:** Formal analysis, Investigation. **Zi-Yi Wang:** Investigation, Methodology. **Chen-Hui Liu:** Visualization. **Jun-Qin Qiao:** Formal analysis, Funding acquisition, Project administration, Resources, Validation, Writing – review & editing. **Wei-Juan Zheng:** Conceptualization, Supervision. **Hong-Zhen Lian:** Conceptualization, Funding acquisition, Resources, Supervision, Writing – review & editing.

Declaration of competing interest

The authors declare that they have no known competing financial interests or personal relationships that could have appeared to influence the work reported in this paper.

Acknowledgments

This work was supported by the National Key Research and Development Program of China (No. 2021YFF0600800), the National Natural Science Foundation of China (22304075, 22176085 and 21874065). The authors sincerely thank Prof. Dr. Pengchao Li, The First Affiliated Hospital of Nanjing Medical University, for providing human urine samples and giving valuable discussion.

Appendix A. Supplementary data

Supplementary data to this article can be found online at https://doi.org/10.1016/j.aca.2026.345714.

Data availability

Data will be made available on request.

References

[1] Z. Marković-Housley, G. Miglierini, L. Soldatova, P.J. Rizkallah, U. Müller, T. Schirmer, Crystal structure of hyaluronidase, a major allergen of bee venom, Structure 8 (2000) 1025–1035, https://doi.org/10.1016/S0969-2126(00)00511-6.
[2] M. Nukui, K.B. Taylor, D.T. McPherson, M.K. Shigenaga, M.J. Jedrzejas, The function of hydrophobic residues in the catalytic cleft of Streptococcus pneumoniae hyaluronate lyase, J. Biol. Chem. 278 (2003) 3079–3088, https://doi.org/10.1074/jbc.M204999200.
[3] M.J. Jedrzejas, R. Stern, Structures of vertebrate hyaluronidases and their unique enzymatic mechanism of hydrolysis, Proteins: Struct., Funct., Bioinf. 61 (2005) 227–238, https://doi.org/10.1002/prot.20592.
[4] G.H. Tekulu, T. Hiluf, H. Brhanu, E.M. Araya, H. Bitew, T. Haile, Anti-inflammatory and anti-nociceptive property of Capparis tomentosa Lam. root extracts, J. Ethnopharmacol. 253 (2020) 112654, https://doi.org/10.1016/j.jep.2020.112654.
[5] B.P. Toole, Hyaluronan: from extracellular glue to pericellular cue, Nat. Rev. Cancer 4 (2004) 528–539, https://doi.org/10.1038/nrc1391.
[6] K.J. Smith, H.G. Skelton, G. Turiansky, K.F. Wagner, R. the military medical consortium for the advancement of retroviral, hyaluronidase enhances the therapeutic effect of vinblastine in intralesional treatment of kaposi's sarcoma, J. Am. Acad. Dermatol. 36 (1997) 239–242, https://doi.org/10.1016/S0190-9622(97)70288-3.
[7] S. Hautmann, V. Lokeshwar, G. Schroeder, F. Civantos, R. Duncan, R. Gnann, M. G. Friedrich, M. Soloway, Elevated tissue expression of hyaluronic acid and hyaluronidase validates the HA-HAase urine test for bladder cancer, J. Urol. 165 (2001) 2068–2074, https://doi.org/10.1097/00005392-200106000-00072.
[8] V.B. Lokeshwar, M.S. Soloway, N.L. Block, Secretion of bladder tumor-derived hyaluronidase activity by invasive bladder tumor cells, Cancer Lett. 131 (1998) 21–27, https://doi.org/10.1016/S0304-3835(98)00197-9.
[9] D. Schrag, L.J. Hsieh, F. Rabbani, P.B. Bach, H. Herr, C.B. Begg, Adherence to surveillance among patients with superficial bladder cancer, J. Natl. Cancer Inst.: J. Natl. Cancer Inst. 95 (2003) 588–597, https://doi.org/10.1093/jnci/95.8.588.
[10] K. Koo, L. Zubkoff, B.E. Sirovich, P.P. Goodney, D.J. Robertson, J.D. Seigne, F. R. Schroeck, The burden of cystoscopic bladder cancer surveillance: anxiety, discomfort, and patient preferences for decision making, Urology 108 (2017) 122–128, https://doi.org/10.1016/j.urology.2017.07.016.
[11] E. Cao, Y. Chen, Z. Cui, P.R. Foster, Effect of freezing and thawing rates on denaturation of proteins in aqueous solutions, Biotechnol. Bioeng. 82 (2003) 684–690, https://doi.org/10.1002/bit.10612.
[12] A. Dorfman, M.L. Ott, A turbidimetric method for the assay of hyaluronidase, J. Biol. Chem. 172 (1948) 367–375, https://doi.org/10.1016/S0021-9258(19)52721-1.
[13] P.J. Knudsen, J. Koefoed, Viscometric determination of hyaluronidase activity in biological fluids, Scand. J. Clin. Lab. Invest. 13 (1961) 673–682, https://doi.org/10.3109/00365516109137343.
[14] C.P. Commission, Pharmacopoeia of the People's Republic of China, 2020 ed., 2020. Beijing, China.
[15] Z. Zhao, Z. Li, J. Huang, X. Deng, F. Jiang, R.P.S. Han, Y. Tao, S. Xu, A portable intelligent hydrogel platform for multicolor visual detection of HAase, Microchim. Acta 191 (2024) 101, https://doi.org/10.1007/s00604-024-06181-y.
[16] M. Tian, C. Lin, Y. Lin, F. Luo, B. Qiu, J. Wang, Z. Lin, L. Wang, Multicolor biosensor of hyaluronidase by the regulation of enzyme-like catalytic activity of Au nanoclusters through changes in the aggregation state, ACS Appl. Nano Mater. 7 (2024) 5620–5627, https://doi.org/10.1021/acsanm.4c00517.
[17] Q. Chen, S. Rong, Y. Cen, G. Xu, Z. Xie, J. Yang, Y. Sun, Q. Hu, F. Wei, A facile fluorescent sensor based on carbon dots and Fe_3O_4 nanoplates for the detection of hyaluronidase activity, Sens. Actuators B Chem. 346 (2021) 130434, https://doi.org/10.1016/j.snb.2021.130434.
[18] M. Qi, Y. Ke, Y. Li, P. Li, H. Zhou, X. Zhang, J. Chen, J. Meng, Au@Pt nanozyme-based smart hydrogel for visual detection of hyaluronic acid, Sens. Actuators B Chem. 427 (2025) 137144, https://doi.org/10.1016/j.snb.2024.137144.
[19] X. Qiu, F. Wang, X. Gao, H. Zhang, H. Wu, X. Gong, J. Lin, Detection of hyaluronidase in urine using hyaluronic acid-coated silver nanoparticles-based surface-enhanced Raman spectroscopy for the diagnosis of bladder cancer, Talanta 294 (2025) 128139, https://doi.org/10.1016/j.talanta.2025.128139.
[20] W. Wang, P. Luo, J. Wang, M. Hong, F. Lu, R. Zeng, T. Lan, Y. Yuan, Y. Lin, J. Liu, Z. Lin, Homogeneous electrochemiluminescence biosensor for hyaluronidase based on the regulation of hyaluronic acid coating on magnetic nanoparticles, Microchem. J. 207 (2024) 112131, https://doi.org/10.1016/j.microc.2024.112131.
[21] Z. Li, X. Huang, H. Liu, F. Luo, B. Qiu, Z. Lin, H. Chen, Electrochemiluminescence biosensor for hyaluronidase based on the adjustable electrostatic interaction between the surface-charge-controllable nanoparticles and negatively charged electrode, ACS Sens. 7 (2022) 2012–2019, https://doi.org/10.1021/acssensors.2c00801.
[22] Z. Li, J. Zhang, H. Chen, X. Huang, D. Huang, F. Luo, J. Wang, L. Guo, B. Qiu, Z. Lin, Electrochemiluminescence biosensor for hyaluronidase based on the Ru $(bpy)_3^{2+}$ doped SiO_2 nanoparticles embedded in the hydrogel fabricated by hyaluronic acid and polyethylenimine, ACS Appl. Bio Mater. 3 (2020) 1158–1164, https://doi.org/10.1021/acsabm.9b01082.
[23] J. Hu, R. Liao, J. Mao, J. Chen, C. Chen, W. Deng, Y. Tan, Q. Xie, Novel "Signal-On" photoelectrochemical assay by regulating the release of cationic dyes with the utilization of target-specific enzymolysis hydrogels, Microchem. J. 206 (2024) 111350, https://doi.org/10.1016/j.microc.2024.111350.
[24] X. Zhang, S. Zhou, Y. He, H. Zeng, X. Hu, Q. Liang, Y. Huang, Y. Xu, Y. Guo, T. Liu, K. Liang, L. Jiang, B. Kong, Superassembled mesoporous carbon-Fe_2O_3 heterochannels for photothermal-enhanced hyaluronidase sensing, Anal. Chem. 96 (2024) 13971–13979, https://doi.org/10.1021/acs.analchem.4c02753.
[25] W. Ruankham, T. Tantimongcolwat, K. Phopin, J. Bausells, M. Hangouët, M. Martin, N. Zine, A. Errachid, Split aptamers immobilized array microelectrodes for detection of chlorpyrifos pesticide using electrochemical impedance spectroscopy, Sens. Actuators B Chem. 372 (2022) 132614, https://doi.org/10.1016/j.snb.2022.132614.
[26] Z.-X. Li, J.-L. Zhang, J. Wang, F. Luo, B. Qiu, L.-H. Guo, Z.-Y. Lin, A novel enzyme-responded controlled release electrochemical biosensor for hyaluronidase activity detection, J. Anal. Test. 5 (2021) 69–75, https://doi.org/10.1007/s41664-021-00158-z.
[27] R. Apak, A. Üzer, Ş. Sağlam, A. Arman, Selective electrochemical detection of explosives with nanomaterial based electrodes, Electroanalysis 35 (2023) e202200175, https://doi.org/10.1002/elan.202200175.
[28] C. Zhang, K. Yang, Y. Yuan, X. Cao, H. Wang, T. Sakamaki, X. Li, Material modification of electrodes in microbial electrochemical system to enhance electrons utilization on the electrode and its impact on microorganisms, J. Hazard. Mater. 475 (2024) 134908, https://doi.org/10.1016/j.jhazmat.2024.134908.
[29] L. Lei, J. Zhang, W. Zhang, J. Hao, K. Wu, Ultrasensitive carbon nanotube-bridged MXene conductive network arrays for one-step homogeneous electrochemical immunosensing of tumor markers, Biosens. Bioelectron. 263 (2024) 116609, https://doi.org/10.1016/j.bios.2024.116609.
[30] H. Li, W. Lv, Q. Yang, Q. Li, F. Li, Inorganic recognizer-assisted homogeneous electrochemiluminescence determination of organophosphorus pesticides via target-controlled emitter release, J. Agric. Food Chem. 69 (2021) 6087–6095, https://doi.org/10.1021/acs.jafc.1c01006.
[31] S.-H. Wen, N. Wang, Z. Yuan, H. Wu, G. Yan, H. Zhang, S. Yu, J. Ma, Y. Zhou, Detection of arsenate in colored grains using an interference-free dual-signal ratiometric HEC sensor, Food Chem. 475 (2025) 143290, https://doi.org/10.1016/j.foodchem.2025.143290.
[32] J.-C. Bollinger, E.C. Lima, L. Mouni, S. Salvestrini, H.N. Tran, Molecular properties of methylene blue, a common probe in sorption and degradation studies: a review,

Environ. Chem. Lett. 23 (2025) 1403–1424, https://doi.org/10.1007/s10311-025-01856-1.

[33] S. He, K. Lin, S. Cheng, N. Gao, J. Liu, H. Li, Improving trace detection of methylene blue by designing nanowire array on boron-doped diamond as electrochemical electrode, Coatings 14 (2024) 762, https://doi.org/10.3390/coatings14060762.

[34] M. Hayat, A. Shah, J. Nisar, I. Shah, A. Haleem, M.N. Ashiq, A novel electrochemical sensing platform for the sensitive detection and degradation monitoring of methylene Blue, Catalysts 12 (2022) 306, https://doi.org/10.3390/catal12030306.

[35] X. Chen, Q. Huang, S. Ruan, F. Luo, R. You, S. Feng, L. Zhu, Y. Wu, Y. Lu, Self-calibration SERS sensor with "core-satellite" structure for detection of hyaluronidase activity, Anal. Chim. Acta 1227 (2022) 340302, https://doi.org/10.1016/j.aca.2022.340302.

[36] Z. Li, C. Tang, D. Huang, W. Qin, F. Luo, J. Wang, L. Guo, B. Qiu, Z. Lin, Sensitive hyaluronidase biosensor based on target-responsive hydrogel using electronic balance as readout, Anal. Chem. 91 (2019) 11821–11826, https://doi.org/10.1021/acs.analchem.9b02487.